Journal of Power Sources 180 (2008) 185–190

Contents lists available at ScienceDirect

Journal of Power Sources

journal homepage: www.elsevier.com/locate/jpowsour

Short communication

Evaluation of TiO_2 as catalyst support in Pt-TiO_2/C composite cathodes for the proton exchange membrane fuel cell

Sophie von Kraemer[a,*], Kjell Wikander[b], Göran Lindbergh[a], Anders Lundblad[a], Anders E.C. Palmqvist[b,c]

[a] *Applied Electrochemistry, Department of Chemical Engineering and Technology, School of Chemical Science and Technology, KTH-Royal Institute of Technology, SE-100 44 Stockholm, Sweden*
[b] *Applied Surface Chemistry, Department of Chemical and Biological Engineering, Chalmers University of Technology, SE-412 96 Gothenburg, Sweden*
[c] *Competence Centre for Catalysis, Chalmers University of Technology, SE-412 96 Gothenburg, Sweden*

ARTICLE INFO

Article history:
Received 7 December 2007
Received in revised form 12 February 2008
Accepted 15 February 2008
Available online 10 March 2008

Keywords:
Titanium dioxide
Carbon degradation
Cathode performance
Proton exchange membrane fuel cell
Polymer electrolyte fuel cell

ABSTRACT

Anatase TiO_2 is evaluated as catalyst support material in authentic Pt-TiO_2/C composite gas diffusion electrodes (GDEs), as a different approach in the context of improving the proton exchange membrane fuel cell (PEMFC) cathode stability. A thermal stability study shows high carbon stability as Pt nanoparticles are supported on TiO_2 instead of carbon in the Pt-TiO_2/C composite material, presumably due to a reduced direct contact between Pt and C. The performance of Pt-TiO_2/C cathodes is investigated electrochemically in assembled membrane-electrode assemblies (MEAs) considering the added carbon fraction and Pt concentration deposited on TiO_2. The O_2 reduction current for the Pt-TiO_2 alone is expectedly low due to the low electronic conductivity in bulk TiO_2. However, the Pt-TiO_2/C composite cathodes show enhanced fuel cell cathode performance with growing carbon fraction and increasing Pt concentration deposited on TiO_2. The proposed reasons for these observations are improved macroscopic and local electronic conductivity, respectively. Electron micrographs of fuel cell tested Pt-TiO_2/C composite cathodes illustrate only a minor Pt migration in the Pt-TiO_2/C structure, in which anatase TiO_2 is used as Pt support. On the whole, the study demonstrates a stable Pt-TiO_2/C composite material possessing a performance comparable to conventional Pt–C materials when incorporated in a PEMFC cathode.

1. Introduction

Degradation of the catalyst support material in the gas diffusion electrode (GDE) of the proton exchange membrane fuel cell (PEMFC) has been discussed recently [1–6]. Previously Kinoshita [7] and Kinoshita and Bett [8] reported on the corrosion of the catalyst-supporting carbon in the context of phosphoric acid fuel cells (PAFCs). The cathodic PEMFC environment, including high acidity, electrochemical potential, water content as well as O_2 concentration, sets high demands on the catalyst support material [1–3]. The presence of Pt on carbon increases the rate of carbon corrosion significantly [3,5,6]. The corrosion of carbon results in a decreased contact between the support and the Pt catalyst particles, which consequently become more mobile and might form larger Pt aggregates or migrate out of the GDE. Carbon degradation can also cause increased hydrophilicity of the supporting carbon, which results in deteriorated mass-transport properties of the GDE [4]. One current approach for eliminating carbon corrosion is to optimize operation conditions, e.g. avoidance of high humidity levels and high-voltage operation. Another approach is development of more stable supporting carbons, such as graphitized carbon, which previously was developed as a support material for PAFC applications when degradation of the GDEs was observed [1,7].

TiO_2 is interesting to evaluate as catalyst support material not only due to its high stability at PEMFC cathode potentials in hydrous, acidic environment, but also due to recent reports on introducing Ti-containing materials into the electrodes. Substoichiometric Ti_nO_{2n-1} has been reported to perform well as catalyst support in PEMFC cathodes [9] and studies on electrodes, where the Pt has been deposited on C/TiO_2, showed an increased electrochemically active area of Pt deposited on carbon in the presence of TiO_2 [10,11]. Incorporation of TiO_2 in the cathode has shown to improve methanol tolerance [11] and TiO_2 and its proton-conductor properties in nm thick electrode films have been discussed [12,13]. However, when introducing TiO_2 into authentic GDEs the influ-

* Corresponding author. Tel.: +46 8 790 8174; fax: +46 8 108087.
E-mail addresses: sophievk@ket.kth.se (S. von Kraemer), kjell.wikander@borealisgroup.com (K. Wikander), Goeran.Lindbergh@ket.kth.se (G. Lindbergh), lundbla@ket.kth.se (A. Lundblad), adde@chalmers.se (A.E.C. Palmqvist).

0378-7753/$ – see front matter © 2008 Elsevier B.V. All rights reserved.
doi:10.1016/j.jpowsour.2008.02.023

ence on cathode performance has generally been reported without considering parameters such as limited electronic conductivity and electrode stability.

In this paper anatase TiO_2 is studied as Pt support in Pt-TiO_2/C composite GDEs as an approach to improve the PEMFC cathode stability. The addition of carbon as electron-conducting component compensates for the low electronic conductivity of TiO_2. By depositing the Pt nanoparticles on TiO_2 prior to the addition of the carbon material, the amount of Pt in direct contact with the carbon is minimized and the aim is to reduce carbon degradation. A thermal stability study is carried out on a Pt-TiO_2/C composite material, in which the Pt is deposited on TiO_2, and on a conventional Pt–C material. Pt-TiO_2/C electrodes are electrochemically characterized in complete membrane-electrode assemblies (MEAs) and the impact of the carbon fraction and the amount of Pt deposited on TiO_2 are studied. The samples are characterized with transmission electron microscope (TEM) before and after the fuel cell testing.

2. Experimental

2.1. Preparation of Pt-TiO_2

Tetrakisdecylammonium bromide (TDAB, 99%) was purchased from Fluka and hexachloroplatinic acid (H_2PtCl_6, 99.95%), sodium borohydride ($NaBH_4$, 99%) and octylamine (C_8NH_2, 99%) were from Aldrich. The organic solvents (toluene, *n*-heptane and ethanol) were all of analytical grade and purchased from Riedel de Haën. MilliQ water was used in all cases. Anatase TiO_2 (Sachtleben, Hombfine N, 99%, particle size ca. 3–5 nm in diameter and BET = 367 $m^2\,g^{-1}$) was obtained as a fine powder and used as received. Vulcan XC-72 (particle size 20–50 nm and BET = 233 $m^2\,g^{-1}$) was obtained from DeNora. A 20 wt% Pt-Vulcan XC-72 (E-TEK) reference material was used in the thermal long-term stability test described in Section 2.4. The glassware used for chemical synthesis were cleaned in aqua regia and carefully rinsed with large quantities of water and dried before use.

Suspensions of Pt nanoparticles of spherical shape and narrow size distribution were prepared following the phase-transfer synthesis method originally developed by Brust et al. [14] using alkylamine as stabilizing agent. In a typical synthesis based on the procedure described by Wikander et al. [15], 16.4 ml of a 0.125-M H_2PtCl_6 stock solution, diluted with 82 ml H_2O, was added to a closed glass vessel containing 3.42 g TDAB dissolved in 239 ml toluene. Upon continuous stirring of the reaction mixture the Pt(IV) ions were transferred from the aqueous phase to the organic phase by means of the TDAB, which acted as phase-transferring agent and was present in large stoichiometric excess. After 2 h of stirring the aqueous phase had become colorless indicating that all Pt(IV) had been transferred to the organic phase. A solution of 10.25 ml C_8NH_2 in 34.2 ml toluene was added to the reaction mixture and was allowed to homogenize for 15 min before 1.30 g $NaBH_4$ dissolved in 85.4 ml water was added drop wise under continuous stirring. Due to reduction of Pt(IV) ions to metallic Pt the color of the reaction mixture turned from orange to deep brown in short time but the reduction reaction was let to continue under stirring for another 2 h. After the reaction was completed, the organic phase containing the Pt-C_8NH_2 nanoparticles, was collected in a separate vessel and the toluene was removed using a rotovapor. The purification procedure was performed as described previously [15].

The octylamine-stabilized Pt nanoparticles were deposited onto a catalyst support material (TiO_2 or Vulcan XC-72) by slowly adding the desired support powder into a recently prepared Pt nanoparticle dispersion under continuous stirring. After the addition of all support material and 10 min of ultrasonication the slurry was stirred for at least 2 h. The toluene was finally removed by means of a rotovapor and a dry powder was obtained.

For the Pt-TiO_2/C composite samples, the Pt-TiO_2 material was prepared as described above, and then dispersed in *n*-heptane to which Vulcan XC-72 powder (density = 1.8 $g\,cm^{-3}$) was added in an amount corresponding to 30 or 50 vol% relative to the amount of added TiO_2 (density = 4.2 $g\,cm^{-3}$). The addition of *n*-heptane enabled the formation of a slurry without extracting the Pt from the TiO_2 surface. Following 10 min of ultrasonication the slurry was stirred for 2 h and next the *n*-heptane was removed using a rotovapor.

2.2. Preparation of electrodes and MEAs

The electrode inks were prepared by adding 2% Nafion solution (Dupont 5 wt% Nafion solution diluted with appropriate amount of isopropanol) to either Pt-TiO_2 or different mixtures of Pt-TiO_2/Vulcan XC-72. The inks were ultrasonicated, stirred for 4 h and pipetted onto heated Nafion 115 membranes respectively preweighed transparency pieces for determination of Pt content. The Nafion content was 30 wt% in all electrodes and the total Pt weight was 0.04–0.25 mg. An ELAT electrode, serving as counter electrode (CE), was heat-pressed at 130 °C onto the opposite side of the membrane and the MEA was mounted with a Sigracet 25BC gas diffusion layer (obtained from SGL Technologies GmbH) on the working electrode (WE) side in the fuel cell test station. Electrodes for electronic conductivity measurements were prepared by airbrushing onto heated transparency material. The pretreatment of Nafion membranes and electrode airbrushing has been previously described [16,17]. The two series of prepared Pt-TiO_2 based electrodes are shown in Table 1: in series (a) the carbon fraction was varied (0–50 vol%) and in series (b) the Pt amount deposited on TiO_2, i.e. the Pt:TiO_2 ratio, was varied. A Pt-Vulcan XC-72 reference sample was prepared, in which the Pt nanoparticles had been prepared and deposited on the carbon by the same methods as in the case of the TiO_2 samples.

2.3. Materials characterization

A JEOL JEM-1200 EX II TEM instrument operated at 120 kV was used for materials analysis. Specimens of each solid powder were prepared by dispersing small amounts of grinded sample in ethanol. One or two drops of the dispersion were then added onto holey carbon-coated TEM grids (Cu 3 mm, 300 mesh, Pelco) placed on a filter paper, which removed the excess solvents. In the case of the as-prepared Pt nanoparticle dispersions, a few drops of dispersion were placed directly on the TEM grid immediately after completed synthesis and were let to dry. The TEM pictures were used for determination of the theoretical geometrical area of the Pt nanoparticles by measurement of ca. 250 nanoparticles in each sample.

The elemental composition and Pt loading of the prepared materials were analyzed with SEM-EDX using a Leo Ultra 55 FEG SEM equipped with an Oxford Inca EDX system operated at 20 kV with a WD = 10 mm (EDX). Before introducing into the SEM vacuum chamber a small sample amount was fixed onto a stainless steel sample holder by means of silver glue.

The N_2 adsorption and desorption isotherms were recorded at −196 °C using a Micromeritics Tristar on finely grinded samples, which had been degassed under vacuum at 200 °C for at least 2 h to remove adsorbates. The specific surface area was calculated with the BET method using the isotherm data from the relative pressure range of 0.05–0.20 [18].

The macroscopic electronic conductivity of the electrodes was determined by the van der Pauw method, described in detail by Lundblad [17].

Table 1
Data of the two evaluated electrode series, in which (a) the carbon fraction was varied and (b) the Pt:TiO_2 ratio was varied

	Studied parameter	Volume ratio TiO_2:Vulcan XC-72	Pt content on TiO_2 (wt%)	Electronic conductivity[a] ($S\,m^{-1}$)
(a)	Variation of carbon fraction	100:0	8	
		70:30	12	
		50:50	12	
(b)	Variation of Pt% deposited on TiO_2	50:50	5	17
		50:50	12	19
		50:50	32	34
Reference	Pt–C	0:100	10.5	

The Pt–C reference sample was prepared by the same method as the Pt-TiO_2 electrodes.
[a] The macroscopic electronic conductivity is measured for series (b) by the van der Pauw method.

2.4. Thermal stability study

The stability of Pt-TiO_2/C, containing 50 vol% Vulcan XC-72, and commercial Pt-Vulcan XC-72 (ETEK) was evaluated by studying the thermal stability in air according to the method described by Stevens et al., in which a high agreement between the described thermal stability test method and an accelerated electrochemical degradation test was demonstrated [5,6]. Non-modified Vulcan XC-72 was employed as a reference material. The samples were kept in air at 170 °C for ~1000 h and the temperature was then increased to 210 °C for ~4000 h to accelerate the degradation test. The samples were weighed at least once every 1400 h and the weight change was noted.

2.5. Electrochemical characterization

The fuel cell test station used for electrochemical characterization of the electrodes was developed by Ihonen et al. [19]. The absolute clamping pressure over the current collectors, which was controlled by a spring screw, was 4 bar in all measurements. The cell temperature was set at 80 °C, the humidifier temperature was 82 °C and the gas pipes between humidifier and cell were set at 87 °C to avoid water condensation. Humidifiers were purchased from Fuel Cell Technologies Inc. and the measurements were carried out using a PAR 273A potentiostat controlled by Corrware software.

All electrodes were evaluated as PEMFC cathodes by an identical measurement routine, consisting of cyclic voltammetry in N_2, iR correction in a symmetrical hydrogen cell, and fuel cell polarization curves with high and low sweep rates in O_2. This routine was carried out in two cycles and the reported results, originating from the second cycle, are the 100 $mV\,s^{-1}$ cyclic voltammograms and the iR corrected polarization curves, measured with a sweep rate of 10 $mV\,s^{-1}$. The anode CE was employed as reference electrode (RE) in all measurements. The polarization curves were recorded with 100% H_2 flowing over the CE but in the cyclic voltammetry measurements the CE was fed with 5% H_2 in Ar. The presented cyclic voltammograms are corrected for the 45.5 mV shift, due to the lower concentration of H_2 on CE/RE side as calculated by Nernst equation. The area of the hydrogen desorption peak was estimated and the corresponding electrochemically active area was calculated by assuming a H-monolayer on Pt with a charge of 210 $\mu C\,cm^{-2}$.

3. Results and discussion

The main objective of this study was to evaluate if supporting the Pt nanoparticles on TiO_2 would improve the stability of the electrode and whether, by introducing carbon to the Pt-TiO_2, a high cathode performance of the composite electrode could be achieved in combination with an improved stability.

3.1. Structural and compositional characterization

The TEM micrographs, shown in Fig. 1, illustrate the structure of the studied materials from the Pt nanoparticles to the fuel cell tested electrodes. In Fig. 1A Pt nanoparticles deposited onto a TEM grid are shown whereas Fig. 1B and C shows Pt-TiO_2/C samples with 30 and 50 vol% carbon, respectively. The mean Pt particle size was 2.4 ± 0.6 nm and the BET area, determined by gas porosimetry, was 367 and 233 $m^2\,g^{-1}$ for the TiO_2 and Vulcan XC-72 materials, respectively. Fig. 1B and C shows the typical composite electrode structure, where the Pt-TiO_2 aggregates are mixed with Vulcan particles and both phases are embedded in Nafion and surrounded by pores. The figures visualize the percolating carbon network in the electrodes, which contributes to the macroscopic electronic conductivity in the electrode, as well as the Pt-TiO_2 aggregates, which are isolated partly from the electronic conducting carbon network and hence influencing the local electronic conductivity. The Pt content and the geometrical Pt area for each sample are reported in Table 2. Fig. 1C and D illustrates the electrode morphology of the Pt-TiO_2/C sample with 50 vol% carbon before and after fuel cell testing, respectively. The TEM micrographs show well-dispersed Pt nanoparticles deposited on the anatase TiO_2 with only a minor spill-over on the carbon as well as a minor migration of Pt in the sample during fuel cell operation. In contrast, TEM micrographs of samples prepared using rutile TiO_2 (not shown) illustrated major spill-over of Pt nanoparticles from the rutile TiO_2 to the carbon.

3.2. Thermal stability evaluation

The results from the thermal long-term stability test are presented in Fig. 2. The degradation of 20 wt% Pt-Vulcan XC-72 was significant while the Pt-TiO_2/C composite, with a total loading of 10 wt% Pt and 50 vol% C, was highly stable during the thermal treatment of 1000 h in 170 °C followed by 4000 h in 210 °C. The as-obtained Vulcan XC-72, employed as reference sample, showed no trend in loss or gain of weight during the stability test period. The random variation in its weight was likely due to balance equipment inaccuracy, to which the error bars in Fig. 2 refer. Previously, a consumed carbon fraction of ~0.2 for 20 wt% Pt-Vulcan XC-72 and ~0.1 for 10 wt% Pt-Vulcan XC-72 after 900 h in 195 °C has been reported [6]. Stevens et al. reported an agreement between the thermal stability method and accelerated electrochemical stability tests [5]. The thermal stability study indicates therefore high electrochemical stability for the Pt-TiO_2/C composite structure.

3.3. Influence of Pt-TiO_2:C ratio on the PEMFC cathode performance

The electrochemical characterization was carried out in two measurement cycles and overall the electrodes were stable during the 24 h of testing. The electrochemical characteristics for the

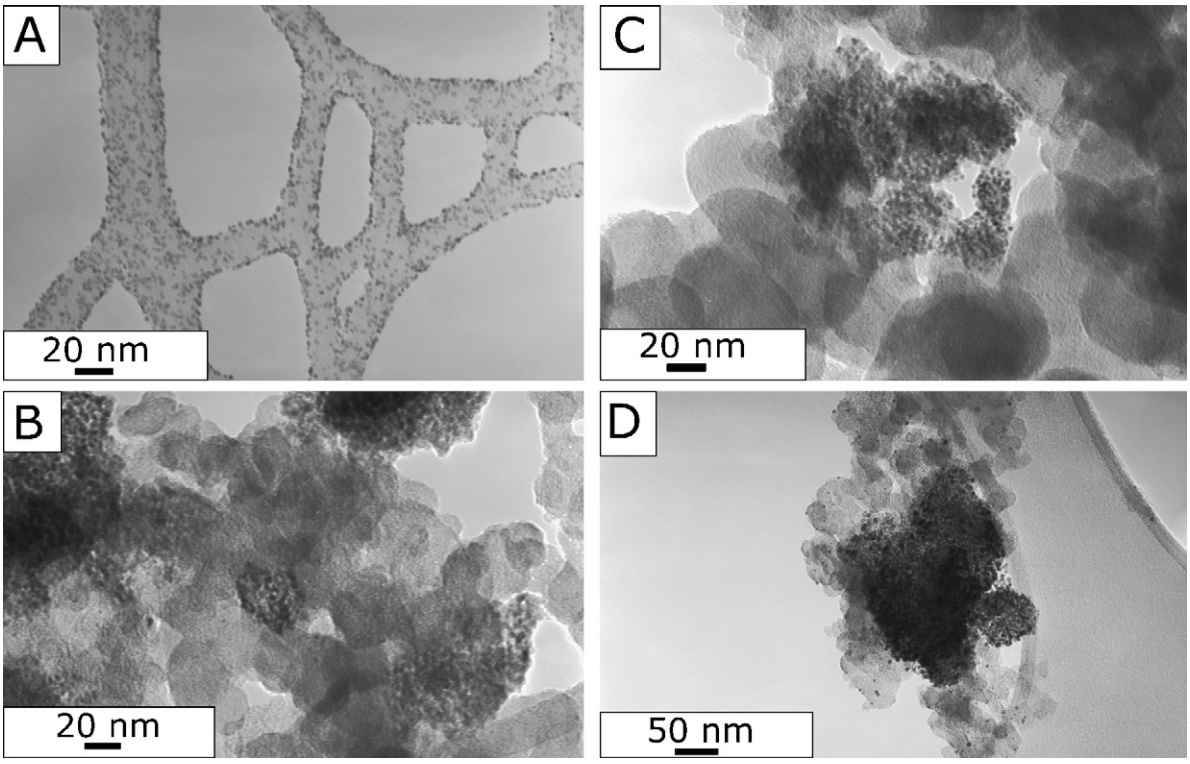

Fig. 1. TEM images of the Pt-TiO_2/C material. In (A) as-prepared Pt nanoparticles deposited directly onto a TEM grid are shown. In (B) and (C) the Pt nanoparticles were deposited on the TiO_2 powder and the Pt-TiO_2 was mixed with Vulcan XC-72 fractions corresponding to 30 vol% carbon and 50 vol% carbon, respectively. In (D) an image of a fuel cell tested Pt-TiO_2/C cathode (50% carbon fraction) illustrates that the catalyst nanoparticles to the most part remain on the TiO_2 support.

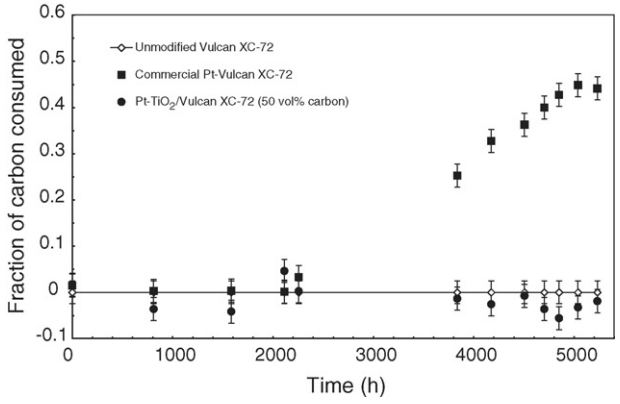

Fig. 2. The thermal stability of unmodified Vulcan XC-72, commercial 20 wt% Pt-Vulcan XC-72 and 10 wt% Pt-TiO_2/Vulcan XC-72 composite material (containing 50 vol% carbon). The temperature was 170 °C for ~1000 h followed by 210 °C for additional ~4000 h.

Pt-TiO_2 based cathodes, with a carbon fraction of 0–50 vol%, are presented in Figs. 3 and 4, which show cyclic voltammograms and polarization curves, respectively. Both figures are normalized to the Pt loading in the cathodes and a Pt–C cathode is presented as reference. The carbon-free Pt-TiO_2 cathode had an expected low electrochemically active area as well as low oxygen reduction activity due to limited macroscopic electronic conductivity of TiO_2. Fig. 3 describes an expected enhanced double layer capacitance in the electrode when the carbon fraction is increased. The increase in the hydrogen desorption peak area illustrates an improved Pt utilization when the fraction of electron-conducting component is increased. The corresponding polarization curves in Fig. 4 show increased ORR current density with increased carbon fraction. The proposed reason for an improved Pt utilization and fuel cell performance due to increased carbon fraction is the establishment of a percolating electron-conducting network in the electrode, which results in an enhanced macroscopic electronic conductivity in the GDE. Nevertheless, also the cathode with 50 vol% carbon is limited at higher current densities despite its sufficiently high macroscopic electronic conductivity, which is discussed further in Section 3.4. The TEM images in Fig. 1 reveal the presence of Pt particles in the TiO_2 aggregates, which are isolated from electron transport, implying that the electrodes are limited by insufficient local electronic conductivity.

3.4. *Influence of Pt:TiO_2 ratio on the PEMFC cathode performance*

The macroscopic electronic conductivity of the Pt-TiO_2/C composite electrodes, containing 50 vol% carbon, was determined by

Table 2
The electrochemically active area and the total geometrical Pt area in the Pt-TiO_2/C composite electrodes

Pt content on TiO_2 support (wt%)	Electrochemically active Pt area[a] (m^2 (g Pt)$^{-1}$)	Geometrical Pt area[b] (m^2 (g Pt)$^{-1}$)
5	8	88
12	14	123
32	17	104
Pt/C sample (10.5 wt% Pt)	29	117

[a] Determined from the hydrogen desorption peak in the cyclic voltammograms.
[b] Calculated from the size histograms based on the TEM micrographs assuming spherical particle geometry.

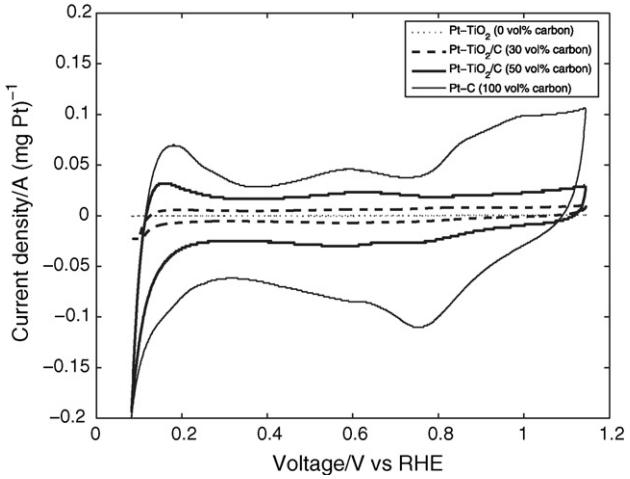

Fig. 3. Cyclic voltammograms show the effect of the increased fraction of added Vulcan XC-72 (0–50 vol%) on the electrochemically active area in the electrodes. The carbon-free cathode has a low active area (hence located close to *x*-axis). The current is normalized to the Pt loading of each sample and the Pt–C reference sample is shown as comparison.

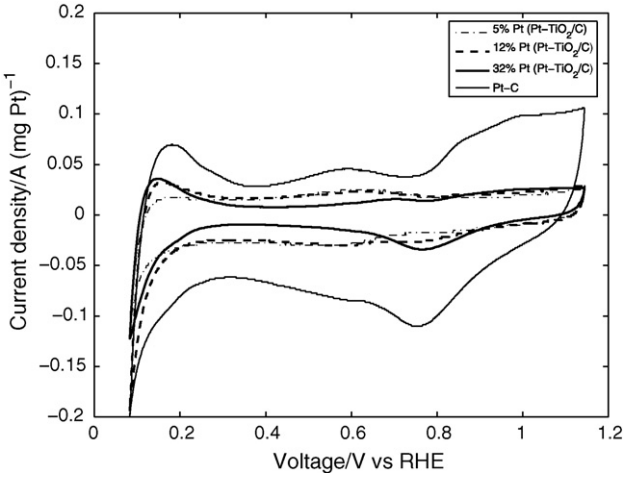

Fig. 5. Cyclic voltammograms of Pt-TiO_2/C composite cathodes, with varying Pt amount deposited on TiO_2, show the electrochemically active area in the electrodes. The curves are normalized to the total Pt content of each sample and all electrodes had a constant carbon content of 50 vol%. The Pt–C reference sample is shown as comparison.

the van der Pauw method and is presented in Table 1. The values are low compared to reported values of 100–400 S m^{-1} for Pt–C based electrodes [16] due to the low bulk electronic conductivity of TiO_2; the band gap of anatase TiO_2 is 3.2 eV [20]. However, the electronic conductivity is considered not to be the limiting parameter when being a factor 5–10 higher than the proton conductivity in a GDE. Typical values for proton conductivity in PEMFC GDEs are in the range of 0.1–0.3 S m^{-1} [16]. Thus a sufficiently high macroscopic electronic conductivity can be assumed in the Pt-TiO_2/C composite electrodes when 50 vol% carbon is present. Carbon creates a percolating electron-conducting network in the electrode, which is also illustrated in Fig. 1C. It should be pointed out that a possible deficiency in local electronic conductivity in the Pt-TiO_2 aggregates is not detectable in the macroscopic electronic conductivity measurements.

Figs. 5 and 6 present the cyclic voltammograms and the fuel cell polarization curves for cathodes, with a constant 50 vol% carbon fraction and a varying Pt amount deposited on TiO_2. The cyclic voltammograms and the polarization curves are normalized to the total Pt content of each sample. The electrochemically active area was determined from the cyclic voltammograms and compared to the calculated total geometrical surface of the Pt nanoparticles based on the TEM analysis (Section 2.3). The results are summarized in Table 2 and overall the electrochemically available area was low in the cathodes compared to the initial geometrical Pt area. The electrochemically active area for the Pt–C reference sample was 29 m^2 g^{-1}, which is in agreement with previous results on similar materials that indicate low Pt utilization [21]. Increased amount of Pt deposited on TiO_2 enhanced the electrochemically active area in the cathode, however the Pt utilization was low in all Pt-TiO_2/Vulcan composite electrodes compared to the Pt–C sample. Fig. 6 illustrates that increased Pt concentration on TiO_2 resulted in increased ORR current and this may be explained by enhanced local electronic conductivity in the Pt-TiO_2 aggregates, which are partly isolated from the percolating electron-conducting carbon network seen in Fig. 1. The likelihood of improved performance, due to a significant increase in the direct contact of Pt–C when the

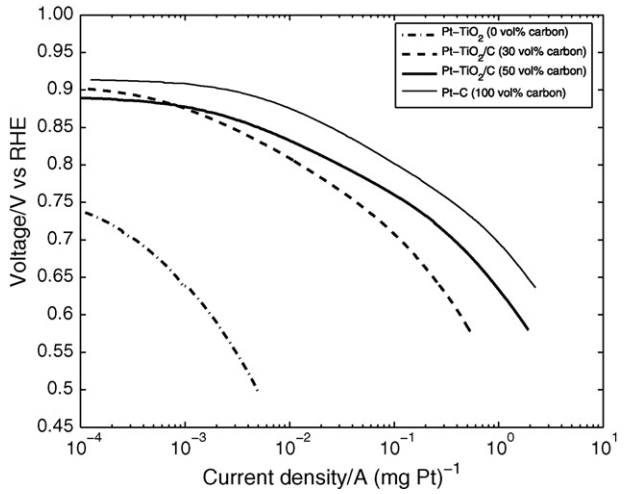

Fig. 4. The polarization curves present the cathode performance dependency on the carbon fraction (0–50 vol%) added to the original Pt-TiO_2 material. The polarization curves are iR corrected and the measured current is normalized to the Pt loading of each sample. The Pt–C reference sample is shown as comparison.

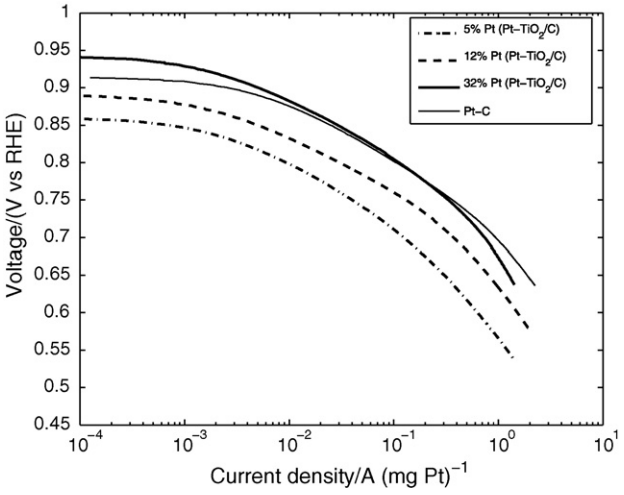

Fig. 6. Polarization curves of a cathode series, in which the Pt amount deposited on the TiO_2 was varied. The carbon fraction was kept constant at 50 vol% and the ORR current of the reference sample based on Pt–C is shown as comparison. The polarization curves are normalized to the total Pt content. The Pt–C reference sample is shown as comparison.

Pt:TiO_2 ratio is increased, can be ruled out by the TEM examination, which illustrates a low degree of direct contact between Pt and C in the Pt-TiO_2/C composite structure throughout the electrode series. The Pt-TiO_2/C composite cathode with highest Pt:TiO_2 ratio possessed a performance comparable to the Pt–C cathode. Further, improvement of cathode performance by electrode ink optimization is expected since the ink compositions used so far have been optimized for Pt–C GDEs [16].

4. Conclusions

TiO_2 was evaluated as cathodic catalyst support material in Pt-TiO_2/C composite GDEs as an approach to improve cathode stability and simultaneously maintain sufficient cathode performance. Small and homogenous Pt nanoparticles were synthesized with the phase-transfer method and deposited on anatase TiO_2. TEM pictures showed highly dispersed and stable Pt particles on the TiO_2 surface. The thermal stability study showed a high stability of the Pt-TiO_2/C composite material, presumably due to a reduced direct contact between Pt and C in the composite structure. In addition, a stable Pt-TiO_2/C composite structure, with only minor migration of Pt during fuel cell operation, was shown by means of post-PEMFC TEM analysis. It was found that the Pt-TiO_2/Vulcan XC-72 composite electrodes possessed improved fuel cell cathode performance when the carbon fraction and the amount of Pt deposited on TiO_2 were increased. The proposed reasons are establishment of a percolating electron-conducting network and increased local electronic conductivity, respectively. On the whole, the study demonstrates a stable Pt-TiO_2/C composite material possessing a cathode performance comparable to conventional Pt–C materials when incorporated in a PEMFC GDE.

Acknowledgements

The financial support from the Swedish Foundation for Strategic Environmental Research, MISTRA, via the program “Fuel cells in a sustainable society” is gratefully acknowledged. A.E.C. Palmqvist thanks the Swedish Research Council for a Senior Researcher grant. Dr. Henrik Ekström at Applied Electrochemistry (KTH) is acknowledged for valuable discussions during the study.

References

[1] M.F. Mathias, R. Makharia, H.A. Gasteiger, J.J. Conley, T.J. Fuller, C.J. Gittleman, S.S. Kocha, D.P. Miller, C.K. Mittelsteadt, T. Xie, S.G. Yan, P.T. Yu, Electrochem. Soc. Interface (Fall) (2005) 24–35.
[2] X. Yu, S. Ye, J. Power Sources 172 (2007) 145–154.
[3] L.M. Roen, C.H. Paik, T.D. Jarvi, Electrochem. Sol. State Lett. 7 (2004) A19–A22.
[4] K.H. Kangasniemi, D.A. Condit, T.D. Jarvi, J. Electrochem. Soc. 151 (2004) E125–E132.
[5] D.A. Stevens, M.T. Hicks, G.M. Haugen, J.R. Dahn, J. Electrochem. Soc. 152 (2005) A2309–A2315.
[6] D.A. Stevens, J.R. Dahn, Carbon 43 (2005) 179–188.
[7] K. Kinoshita, Carbon Electrochemical and Physiochemical Properties, John Wiley & Sons, New York, 1988, pp. 319–334.
[8] K. Kinoshita, J. Bett, Carbon 11 (1973) 237–247.
[9] T. Ioroi, Z. Siroma, N. Fujiwara, S. Yamazaki, K. Yasuda, Electrochem. Commun. 7 (2005) 183–188.
[10] J. Shim, C.-R. Lee, H.-K. Lee, J.-S. Lee, E.J. Cairns, J. Power Sources 102 (2001) 172–177.
[11] L. Xiong, A. Manthiram, Electrochim. Acta 49 (2004) 4163–4170.
[12] H. Ekström, B. Wickman, M. Gustavsson, P. Hanarp, L. Eurenius, E. Olsson, G. Lindbergh, Electrochim. Acta 52 (2007) 4239–4245.
[13] M. Gustavsson, H. Ekström, P. Hanarp, L. Eurenius, G. Lindbergh, E. Olsson, B. Kasemo, J. Power Sources 163 (2007) 671–678.
[14] M. Brust, M. Walker, D. Bethell, D.J. Schiffrin, R. Whyman, J. Chem. Soc., Chem. Commun. 7 (1994) 801–802.
[15] K. Wikander, C. Petit, K. Holmberg, M.-P. Pileni, Langmuir 22 (2006) 4863–4868.
[16] P. Gode, F. Jaouen, G. Lindbergh, A. Lundblad, G. Sundholm, Electrochim. Acta 48 (2003) 4175–4187.
[17] A. Lundblad, J. New Mater. Electrochem. Sys. 7 (2004) 21–28.
[18] S. Brunauer, P.H. Emmet, E. Teller, J. Am. Chem. Soc. 60 (1938) 309–319.
[19] J. Ihonen, F. Jaouen, G. Lindbergh, G. Sundholm, Electrochim. Acta 46 (2001) 2899–2911.
[20] A. Fujishima, K. Hashimoto, T. Watanabe, TiO_2 Photocatalysis—Fundamentals and Applications, BKC Inc., Tokyo, 1999.
[21] K. Wikander, H. Ekström, A.E.C. Palmqvist, G. Lindbergh, Electrochim. Acta 52 (2007) 6848–6855.